Chapter 5

Synthesis, Characterization and Application of Silver and Gold Nanoparticles capped with Diethylenetriaminepentaacetic acid (DTPA) for Chromium sensing

5.1 Introduction

Chromium is extensively used and exists abundantly in two oxidation states i.e. Cr^{3+} and Cr^{6+}, which are both toxic, but Cr^{6+} is the primary subject of concern for various international environmental agencies because it has more mutagenic properties than Cr^{3+}. The maximum permissible concentration of Cr^{6+} in drinking water according to the US Environmental Protection Agency is 0.1 mg/L, which is one reason why the accurate determination of Cr^{6+} levels is very important in water analysis. Hence, the need to develop rapid, sensitive, and reliable methods for chromium detection as more convenient approaches for field assays is of interest.

Recently, various noble metal nano particles (NPs) have been widely used as attractive colorimetric or surface-enhanced Raman scattering probes because of their strong surface plasmon resonance (SPR) absorption properties, high extinction coefficient in the visible region and color-tunable behavior that depends on size, shape, and interparticle distance (Arakawa & Kawasaki, 2010; Burda, Chen, Narayanan, & El-Sayed, 2005; X. Wang, Chen, & Chen, 2014).

Gold nanoparticles (Au NPs) and silver nanoparticles (Ag NPs), have been of particular interest as probes in detection of metal ions and bio molecules because of various advantages such as no requirement of sophisticated materials and complex instruments, ability to detect with naked eyes, and high stability (Lai & Tseng, 2011; Rattanarat et al., 2013; W. Ren, Zhu, & Wang, 2012; Y. Wang, Yan, & Chen, 2013; Y. Xu, Yang, Zhu, & Dou., 2014).

However, in most cases nano sized metal particles in the solution can agglomerate due to Vander Waals forces and high surface energy unless they are protected. In this regard, surface modification using polymers, complex ligands, or surfactants is required to stabilize metal NPs (Ahmadi, Wang, Green, Henglein, & El-Sayed, 1996; Pal, Sau, & Jana, 1998). NP surfaces are generally capped with a surface monolayer of different composition from that of nanoparticle itself (Brust, Walker, Bethell, Schiffrin, & Whyman, 1994; Yonezawa & Kunitake, 1999). This layer is necessary to prevent the NPs from aggregating when suspended in a liquid, and it can also serve as a platform for the attachment of other molecules. Sulfur ligands other than thiols, such as Xanthates (Tzhayik, Sawant, Efrima, Kovalev, & Klug, 2002), Disulfides (Tzhayik et al., 2002), Thioethers (Shelley et al., 2002) Carbamate (Zhao, Jin, Yan, Liu, & Zhu, 2012) have also been widely used as surface functionalization groups for gold.

Triazole-ester and carboxyl-, glutathione-, calixarene-modified Ag NPs have been used as colorimetric probes for sensing of various pollutants (H. Li, Cui, & Han, 2009; H. Li, Yao, Han, & Zhan, 2009; Xiong & Li, 2008; Yao, Tian, & Li, 2010). It has been reported that amino polycarboxylic acids have good reducing and complexing properties. There are a number of reports in the literature in which the metal NPs have been synthesized using complexes of polyaminocarboxylic acids which include Ag-EDTA and Ag-DTPA. In most of these studies, reduction was carried out either by strongly reducing free radicals generated by aqueous radiolysis (Kapoor & Mukherjee, 2003) or by boiling the solution in autoclave at high temperature (Cavicchioli, Varanda, Massabni, & Melnikov, 2005; Hsieh, Pan, & Chen, 2011; Jiang et al., 2011; Yi et al., 2011; Zainy et al., 2012). However, very few studies exist in the literature in which reduction of Ag complexes was carried out without using any reducing agent (Guo, Zhang, Zhu, & Jiang, 2008; Wrzesien & Graham, 2012; Yang & Sardar, 2011) APCAs such as ethylenediaminetetraacetic acid (EDTA) (Bonggotgetsakul, Cattrall, & Kolev, 2011; D. . Wang, Liu, Zhou, Sun, & You, 2007) and Nitrilotriacetic acid (Njagi & Goia, 2014) are also used for reduction of $HAuCl_4$ to form gold nano particles; In their report, "formation of silver nanoparticles in the presence of complexons of Aminopolycarboxylic Acids family". Shevchenko et al. reported that silver nanoparticles can be formed using DTPA without any reducing agents (Shevchenko, Zhuravkov, & Novikov, 2015).

In this work, DTPA was chosen for preparation of capped Ag and Au NPs based on the hypothesis that DTPA contain five carboxyl groups, which suggests that they can serve as an effective capping ligands like citrate. (Ji et al., 2007).Further, DTPA can also bind to NP surface due to the interaction between one carboxyl group of DTPA and metal surface and the negatively charged carboxyl group can stabilize the NPs against aggregation as well as help in binding to chromium. DTPA can act as both reducing agent and capping agent for stabilization of Au and Ag NPs.

Generally the synthesis of NPs has been performed at high tempertaures.. Now a days, microwave irradiation (MWI) is considered as a highly effective technology and is used widely in the synthesis of nanoparticles since it has a more homogeneous heating process and can speed up the reaction rate by many orders of magnitude compared with conventional heating (Bahadur et al., 2011; Jiang et al., 2013).

Our objective of this work was to synthesize DTPA capped Ag and Au nanoparticles using microwave radiation and carrying out their application for the sensing of Cr^{6+} and Cr^{3+} ions in aqueous solutiom.

5.2 Materials and Methods

5.2.1 Materials

$AgNO_3$ (Silver Nitrate, SRL, India), $HAuCl_4$ (Chloroauric Acid, Spectrochem, India) and DTPA (Diethylenetriaminepentaacetic acid, Spectrochem, India). Microwave oven (ONIDA, Power Convention 20, MO20C1S26S (20L)). $AgNO_3$ and $HAuCl_4$ were prepared were in DM water, while DTPA was prepared in 0.2M NaOH.

5.2.2 Synthesis of Ag-NPs and Au-NPs

Microwave Technology was used for synthesis of Silver and Gold NPs. For this synthesis all glassware were thoroughly cleaned with aqua-regia (3:1 HCl/HNO_3) and rinsed with Double distilled water prior to use. The low vacuum MW reactor was a home-appliance kitchen microwave from Onida Power Convection 20 (Model no : MO 20CJS 26S) system with power of 1350 W.

The synthesis of AgDTPA and AuDTPA NPs was carried out under MW irradiation for 1.5 min with a pulse-mode (i.e., irradiation for 30 s and pause for 10 s) and finally cooled down to 25 ℃

5.2.2.1 AgNPs with DTPA

About 0.5mL 0.04M $AgNO_3$ solution was added to 50ml Double distilled water in reaction glass vessel to which 0.5ml of 0.05M DTPA in 0.2M NaOH solution was added . The pH of solution was adjusted to 8.8-9.2 using 0.01M solution of NaOH and heated in microwave. Deep yellow colored AgNP solution was formed which was cooled to room temperature.

5.2.2.2 AuNPs with DTPA

About 0.1mL of 0.02M $HAuCl_4$ solution was added to 5 mL Double distilled water in a glass beaker followed by 0.1mL of 0.05M DTPA. The pH of solution was adjusted to 8.8-9.2 using 0.01M solution of NaOH and heated in microwave for 1.5 min and allowed to cool to room temperature. The colour of solution turned to wine red, which suggested the formation Au NPs.

5.2.3 Characterization Techniques

UV-Visible spectral analysis was carried out using a (JASCO,V-630) spectrophotometer. The morphology of nanoparticles were characterized by using a Tecnai 20 transmission electron microscope (TEM) from Philips Holland, equipped with Electron Source as W emitter and LaB6 (Magnification : 25x to 750000x or higher). Raman analysis was carried out on NXR FT-Raman Module from Thermo scintific, scanning from 200-2000 cm^{-1}. Zeta potential analysis was carried out using Brookhaven 90Plus, particle Size Analyzer.

5.3 Results and Discussion

5.3.1 UV-Visible spectroscopic studies

The formation of AgNPs was accompanied with appearance of intense absorption peak at 400 nm which was attributed to surface plasmon resonance phenomena of electrons in the conduction bands of silver and indicated the formation of silver colloids with nanometer-sized dimensions (Zhang, Li, Goebl, Lu, & Yin, 2011). The single dipole plasmon resonance peak at 400 nm is characteristic of spherical Ag nanoparticles (Bai et al., 2013; S. Xu et al., 2011). The gold nanoparticles formed in the present work had absorbance maxima at 520nm (Figure 5.1).

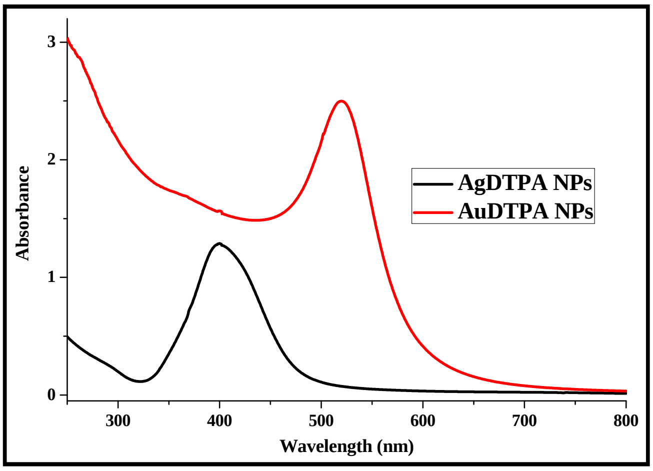

Figure 5.1 UV-Visible spectral analysis of AgDTPA and AuDTPA NPs

5.3.2 Optimization of the reaction conditions

5.3.2.1 Effect of pH

pH was observed to be a crucial factor in the synthesis of nanoparticles. pH values higher than 6.0 were conducive to formation of stable AgNPs in solution (Figure 5.2).. When the pH is higher than 6.0, the AgNPs were stable over one week. However, when the pH was lower than 5.0, with time a slight shift of the extinction band and modest colour change were observed.

Figure 5.2 showed the pH-dependent formation of AuNPs. The nano particles seemed to form from pH 5. Here the UV-vis spectrum displayed a prominent absorbance shoulder at long wavelengths. The absorption was attributed to a dipole like plasmon resonance from gold nanoparticle pairs and was a' hallmark of aggregation' (Kim, Lee, Gong, & Joo, 2005). The 289 nm absorption band as a shoulder attributed to $p_{\sigma} \rightarrow 5d_{x2-y2}$ transitions in the square planar $AuCl_4^-$ complex ion (Andreescu, Sau, & Goia, 2006) was also seen at lower pH conditions of 5-8 and disappeared at pH 10 to 11 when a plasmon peak of wine red gold nanoparticles was observed at 520 nm.

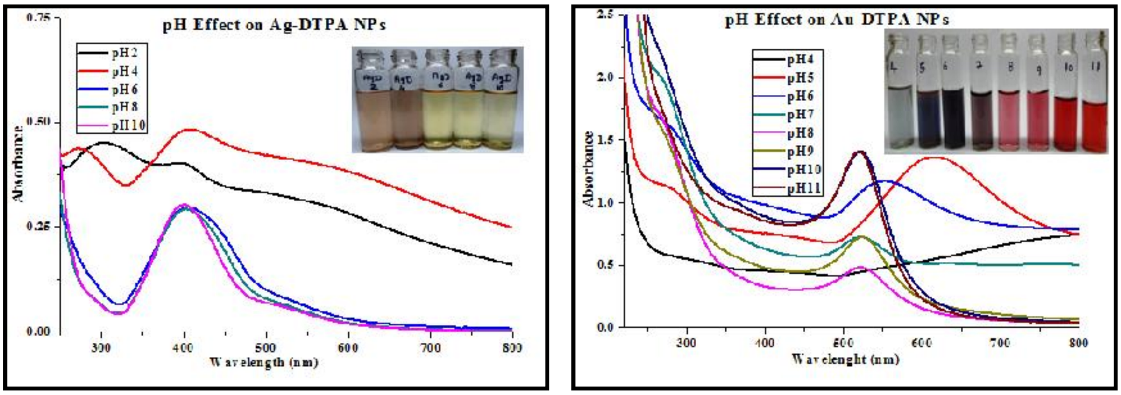

Figure 5.2 Effect of pH on formation of Ag-DTPA and Au DTPA NPs

5.3.2.2 Effect of DTPA concentration

It was observed (Figure 5.3) that in the case of AgNPs the effective formation of NPs occurred at 0.05 M DTPA.

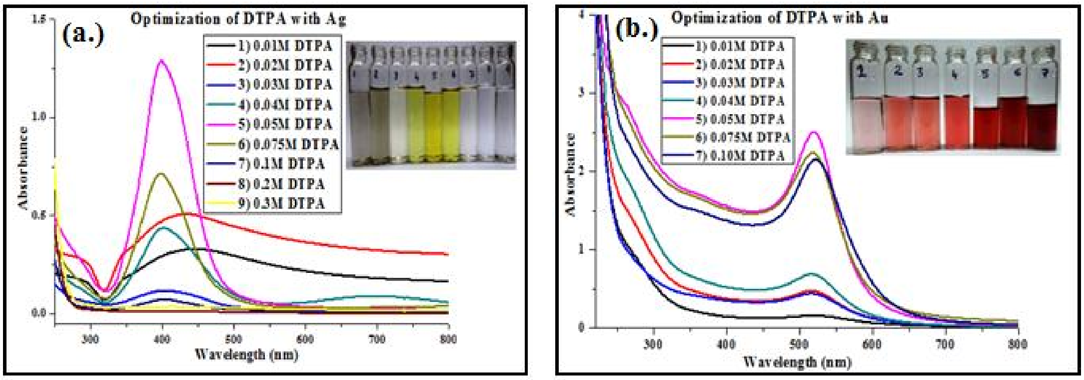

Figure 5.3 Effect of DTPA concentration on formation of a) AgNPs and b) AuNPs

a) DTPA - 0.01- 0.3 M $AgNO_3$ - 0.04M, pH-6 Total volume- 50 ml

b) DTPA - 0.01-0.1M $HAuCl_4$ - 0.02M, pH-8, Total volume- 5.0 ml.

The NPs formed were of reduced intensity when DTPA concentration was 0.03-0.04 M. At lower concentrations proper AgNPs formation did not occur. Surprisingly AgNPs did not form when DTPA concentration was higher than 0.05 M. Probably higher DTPA concentration led to the formation of stable silver complex and reduction could not occur (Chadha, Das, Maiti, & Kapoor, 2014).

In the case of AuNPs, effective formation of AuNPs was observed with 0.05 M DTPA and absorbance slightly decreased when DTPA concentration was increased to 0.075 and 0.1 M. The colloid stabilization properties of DTPA were caused likely, as in the case of the citrate and NTA, by the ability of the carboxylic groups in the molecule to strongly attach to the surface of Ag/Au NPs(Njagi & Goia, 2014).

5.3.2.3 Effect of $AgNO_3$ / $HAuCl_4$ concentration

Figure 5.4 a and b show photographic images of AgNPs formed using different concentrations of $AgNO_3$, viz (0.01 to 0.1 M) and AuNPs formed using different concentrations of $HAuCl_4$ (0.005 to 0.02M) respectively. The color changes significantly when 0.01M $AgNO_3$ was added to the alkali dissolved 0.05M DTPA; the color becomes more intensive and darker upon increasing $AgNO_3$ concentration. The color turned to yellow with 0.03 M $AgNO_3$ and was brown at 0.05M. The absorbance of this solution was high and had to be diluted 10 times wherein the absorbance was ~1.3. The dark colored solution at higher concentrations of $AgNO_3$ after dilution in distilled water was brown even for highest concentration and had the same absorbance maxima but was a broad peak of reduced intensity when diluted 10 times for 0.1M $AgNO_3$ suggesting formation of AgNPs of different sizes as well as aggregation.

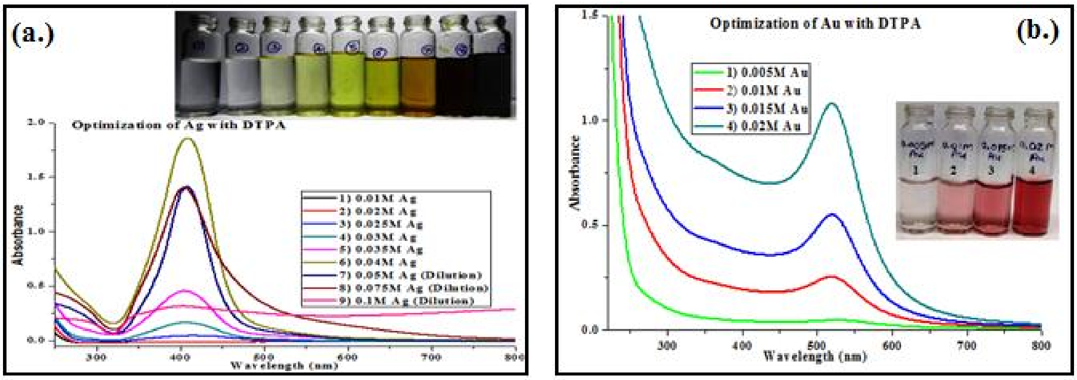

Figure 5.4 Optimization of AgNO3/$HAuCl_4$

a) Ag-DTPA NPs - 0.05M DTPA, pH-6 Total volume. 50 ml

b) Au DTPA NPs- 0.05M DTPA, pH-8 Total volume. 5ml

The increase in absorbance and a relatively sharp absorption spectrum when 0.04-0.075M $AgNO_3$ was used was certainly, a manifestation of increased magnitude of AgNPs formation which reflected the powerful reduction ability of DTPA.

The concentration of $HAuCl_4$ was varied from 0.005 to 0.02 M and the absorption spectrum was monitored to study the formation of nano-gold particles(Figure 5.4 b). The maximum amount of AuNPs formation was observed at 0.02 M $HAuCl_4$ concentration.

5.3.2.4 Effect of temperature

For synthesis of NPs, different thermal techniques including reflux, microwave and room temperature were employed. Microwave Conditions gave appropriate results. The conditions for microwave synthesis for Ag DTPA NPs and Au DTPA NPs was power setting of 917 W for irradiation for 30 s and pause for 10 s. The temperature conditions were very critical for the formation of DTPA capped AgNPs and AuNPs.

5.3.3 TEM Analysis

Transmission electron microscopy (TEM) analysis was carried out to study the size and shape of prepared NPs.

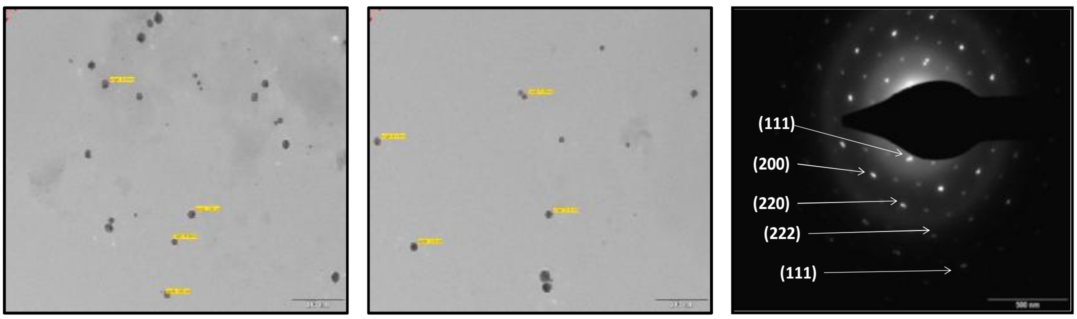

Figure 5.5(a) TEM images of Ag-DTPA NPs

Typical TEM image of as synthesized DTPA capped silver nano particles presented in figure 5.5 a showed non agglomerated, well dispersed AgNPs, with size ranging from 19 to 30 nm (Figure 5.5a) while in the case of gold more uniform DTPA capped Au NPs in the range 7 to 13 nm (Figure 5.5b) were obtained in accordance with observations made by Haiss et al that gold nano particles of this size range showed absorbance maximum in the range 520-525nm (Haiss, Thanh, Aveyard, & David G. Fernig, 2007). The dual role action of alkali treated DTPA toward reducing Ag^+ to Ag^0 as well as gold and stabilization via capping during the preparation process is thus established. The clear lattice fringes in the selected area diffraction pattern confirms the presence of polycrystalline DTPA capped AgNPs (Figure 5.5 a) in the sample while the crystallinity was relatively lesser in DTPA capped AuNPs (Devi & Joshi, 2015). Majority of the AuNPs are spherical in shape (Figure 5.5 b).

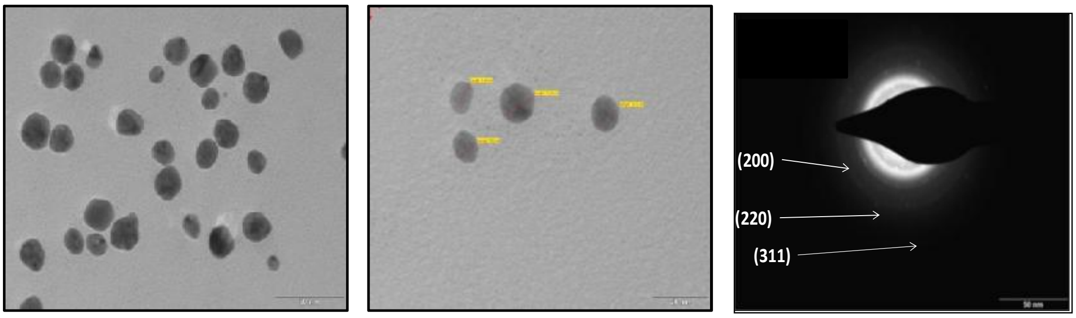

Figure 5.5(b) TEM images of Au-DTPA NPs

The Diffraction rings patterns can be seen very clearly in Ag DTPA which could be identified as (111), (200), (220), (222) and (311) planes while they are not seen clearly in Au DTPA. However the planes could be identified as (200), (220) and (311).

5.3.4 Stability with Time

The stability of the synthesized nanoparticles stored at ambient temperature was examined by running the optimized procedure described in section 5.3.1.

It was observed that AgNPS were less stable (one week) as compared to AuNPs(more than one month)

5.3.6 Zeta Potential Analysis

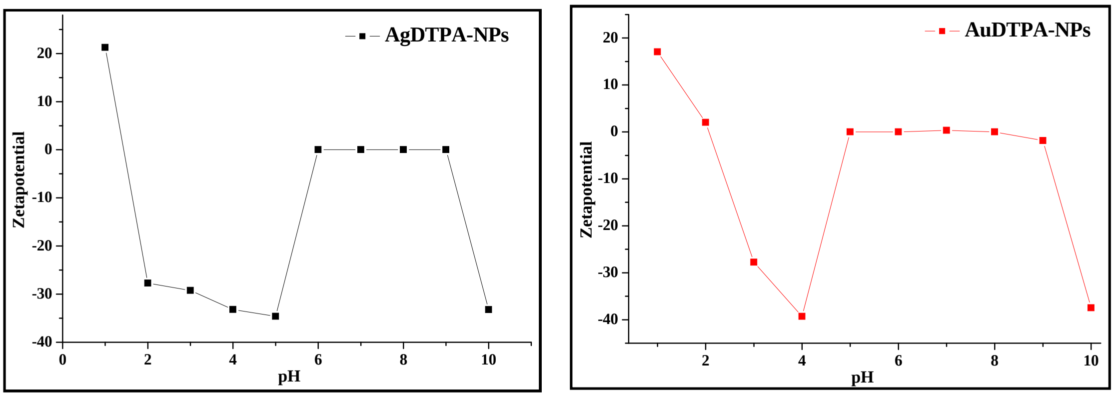

Figure 5.8 Zetapotential images of AgDTPANps and AuDTPANps

The nanoparticles have zero point charge around pH 5 to 9 and 6 to 9 for AgDTPA and Au DTPA NPs. But the nanoparticles are stable because of the zwitter ionic nature of DTPA with three amine nitrogen atoms and five carboxylate atoms (Svanedal et al., 2014).

5.4 Sensing of chromium ion using Ag-DTPA/ Au-DTPA

To investigate the ability of Ag/ AuNPs for the detection of metal ions in aqueous solutions, various toxic metal ions were treated with Ag/ AuNPs and the colorimetric responses were monitored and their UV-Vis absorbance spectra were recorded and analyzed. Ag and AuNPs showed a high selective quenching effect toward Cr^{3+} ions and enhance absorbance in the presence of Cr^{6+} against all the other metal ions tested, which suggested its potential as a Chromium sensor.

5.4.1 Evaluation of sensing potential of Ag-DTPA/ Au-DTPA

To evaluate the response of Au-DTPA NPs toward various metal ions, the absorption spectra of Au-DTPA NPs were taken in the presence of several metal ions (in 1 mM solutions): Ba^{2+}, Cd^{2+}, Co^{2+}, Cu^{2+}, Hg^{2+}, Mg^{2+}, Na^{+}, Pb^{2+}, Cr^{3+} and Cr^{6+}. Figure 5.10 showed the effect of metal ions on the SPR of AgDTPA NPs and AuDTPA NPs in aqueous solution. It is evident that Cr^{3+} and Cr^{6+} were the only metal ion that caused the aggregation of AgDTPA NPs and AuDTPA NPs. It is also evident from Figure 5.10 that no aggregation of Au-DTPA NPs was observed in case of other metal ions except Cr^{3+} and Cr^{6+}.

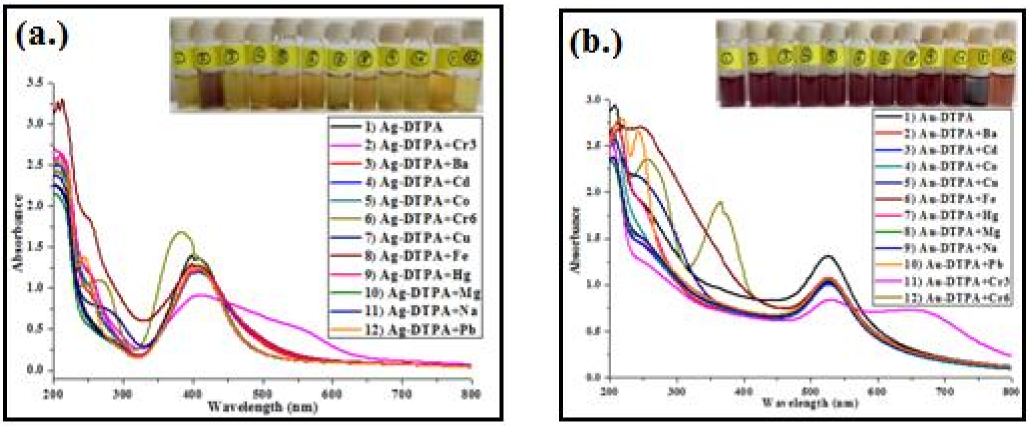

Figure 5.9 Sensing potential of (a) Ag-DTPA (b) Au-DTPA towards various metal ions

Cr^{3+} and Cr^{6+} resulted in additional peaks in the absorbance spectrum of AuDTPA NPs. An additional peak for Cr^{3} was observed at 670 nm and at 365 nm on addition of Cr^{6+} while the absorbance decreased for Cr^{3+} and increased for Cr^{6+} at 525 nm. Other metal ions did not influence the absorption spectra, indicating that no aggregation occurred.

Addition of Cr^{3+} ion to AgNPs resulted in an absorption peak shift, from 410 nm to 549 nm and a decrease in absorbance at 400 nm. This red shift could also be observed by the naked eye as a color change from red to blue while Cr^{6+} ion to AgNPs resulted in an absorption peak shift, from 400 nm to 390 nm with decrease in absorbance at 365 nm. The color change is not visible clearly in the inset images. Other metal ions did not influence the absorption spectra, indicating that no aggregation occurred.

These response for Cr^{3+} can be explained on the basis of Mie theory (Mie, 1908). According to Mie theory, when the distance between two nanoparticles becomes smaller than the sum of their radii, the SPR band displays a red shift, broadening and decrease in intensity at the original SPR. When the morphology of ellipsoidal/spherical AgNPs/ AuNPs is changed and , a new absorption peak appears at higher wavelength (Shankar & John, 2015). Thus, both color change and appearance of a new peak at higher wavelength region suggesting the morphological changes of Au-DTPANPs. The red shift in the SPR band was ascribed to the near-field coupling that occurs when the interparticle distance decreases.

To evaluate the mechanism and selectivity of sensing of Cr^{3+} and Cr^{6+} using both AgNPs-DTPA and AuNPs-DTPA, different experiments were carried out by varying concentration of Cr^{3+} and Cr^{6+} and also carrying out sensing of Cr^{3+} and Cr^{6+} in presence of other metal ions. For ease of understanding the studies were discussed separately.

5.4.2 AgNPs-DTPA sensors for chromium (pH-6, $AgNO_3$-0.04M, DTPA-0.05M, Cr^{3+}/Cr^{+6}-1mM)

5.4.2.1 Ag-DTPA NPs Calibration plot of Cr^{3+}

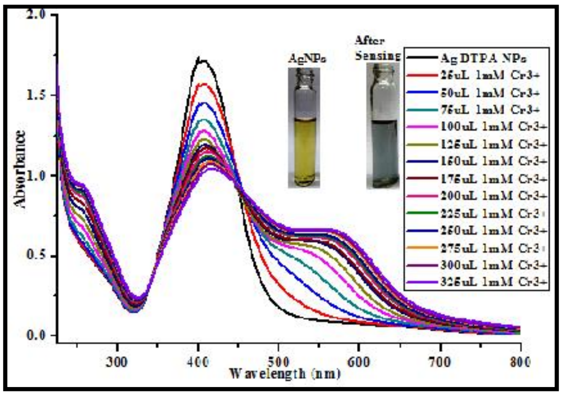

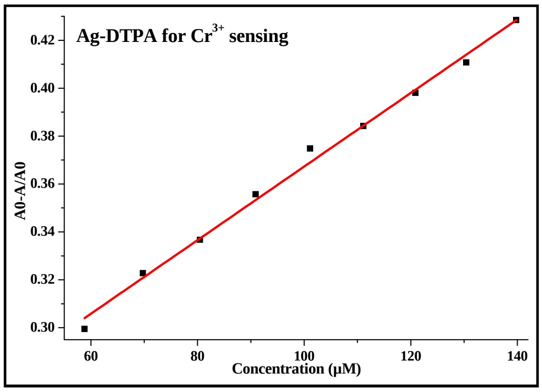

Figure 5.10a concentration variation studies for Cr^{3+}-AgNPs-DTPA sensing

Figure 5.10b linear plot of Cr^{+3} sensing using Ag-DTPA

In this series of studies, the presence of Cr^{3+} led to a marked red-shift of extinction bands**,** with the addition of Cr^{3+}, the absorption band of AgNPs changed gradually from 400 nm to longer wavelengths, finally reaching a maximum at 575 nm and further remained constant. The shift in the surface plasmon resonance peak for AgNPs may be the result of the charge-based interaction between the negatively charged groups of chromium $Cr(OH)_4^-$and positively charged groups of AuNPs DTPA(NR_3^+) as well as hydrogen bonding between $Cr(OH)_4^-$ and COO^- groups of AgDTPA.

The absorbance linearly decreased with increasing concentrations of Cr^{3+} (Figure 5.10b). A calibration graph of Ao-A/Ao vs concn of Cr^{3+} was plotted where Ao is the initial absorbance of NPs under study and A is the absorbance after addition of Cr^{3+} solution of different concentrations·The limit of detection for Cr^{3+} was 1.62 μM. The relationship between absorbance and concentration of Cr^{3+}ions was linear in the 58 μM - 140 μM range

5.4.2.2 Ag-DTPA NPs: Calibration plot of Cr^{6+}

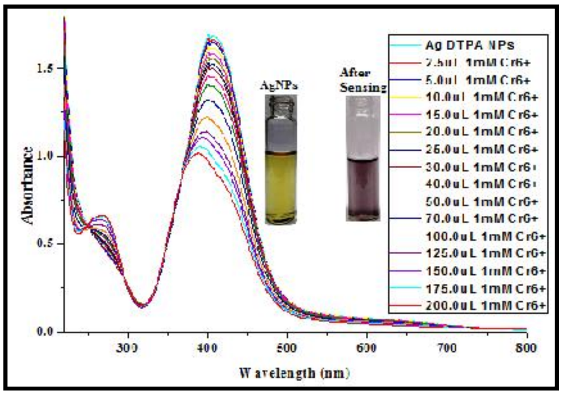

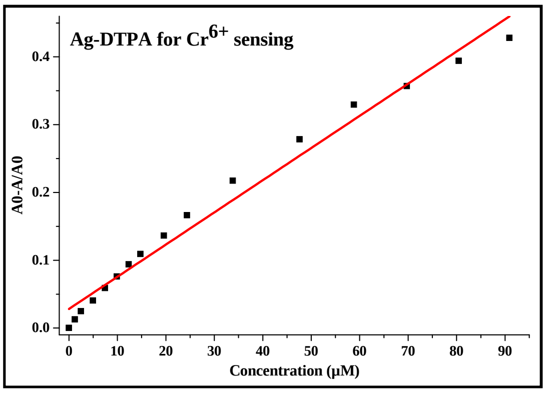

Figure 5.11a concentration variation studies for Cr^{6+}-AgNPs-DTPA sensing

Figure 5.11b linear plot of Cr^{+6} sensing using Ag-DTPA

The initial Ag-DTPA NPs exhibited the SPR absorption peak located at 400 nm and the SPR absorption peak gradually blue shifted and the absorbance decreased as the concentration of Cr^{6+} increased. The isobestic point characteristic of dichromate/ $HCrO_4^-$ was observed at 250 nm.

Under these optimized conditions, the Ag-DTPA NPs were utilized for the colorimetric assay of Cr^{6+}. As shown in Figure 5.11a, various colors of the Ag-DTPA NPs aqueous solutions have been seen after the addition of different concentrations of Cr^{6+}. As the concentration of Cr^{6+} increased from 2.5 uL to 200uL of 1mM, the color of the aqueous solutions gradually changed from yellow to bluish yellow. The color was visibly observed at higher concentrations of change Cr^{6+}. A calibration graph of for Cr^{6+} was plotted as described under section 5.4.2.1 after addition of Cr^{6+} solution of different concentrations. The detection limit of Cr^{6+} was about 1.77 µM, with the linear range 1.24 µM - 90.9 µM (Figure 11b).

5.4.2.3 Ag-DTPA NPs -Effect of other metals on sensing of Cr^{3+} and Cr^{6+}

The selectivity of the AgDTPA NPs sensor for 1mM Cr^{3+}/Cr^{6+} was evaluated by monitoring the absorbance in the presence of 1mM concentration of other metal ions, including Ba^{2+}, Cd^{3+}, Co^{2+}, Cu^{2+}, Fe^{3+}, Hg^{2+}, Mg^{2+}, Na^{+}, Pb^{2+} and Cr^{6+}/Cr^{3+}.The observations are seen from Figures 5.12 for Cr^{3+} and Cr^{6+} respectively

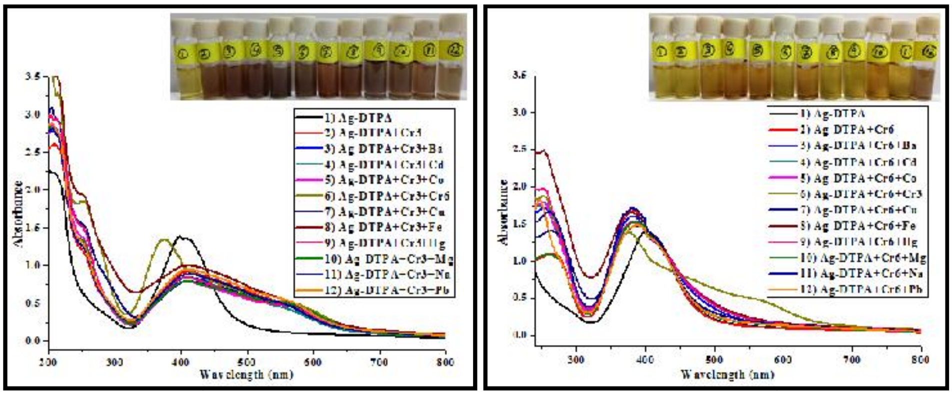

Figure 5.12 Ag-DTPA NPs: Effect of other metal on sensing in presence of Cr^{3+}/Cr^{6+}

It can be seen from Figure 5.12 that only Fe^{3+} and Cr^{6+}/Cr^{3+} showed significant interference during determination of Cr^{3+}/ Cr^{6+}. The AgDTPA NPs would be useful for determination of total chromium selectively.

5.4.3 Au-DTPA NPs as sensors for chromium (pH 8, $HAuCl_4$ 0.02M, DTPA-0.05M, Cr^{3+}/Cr^{+6}-1mM)

5.4.3.1 Au-DTPA NPs Calibration plot for Cr^{3+}

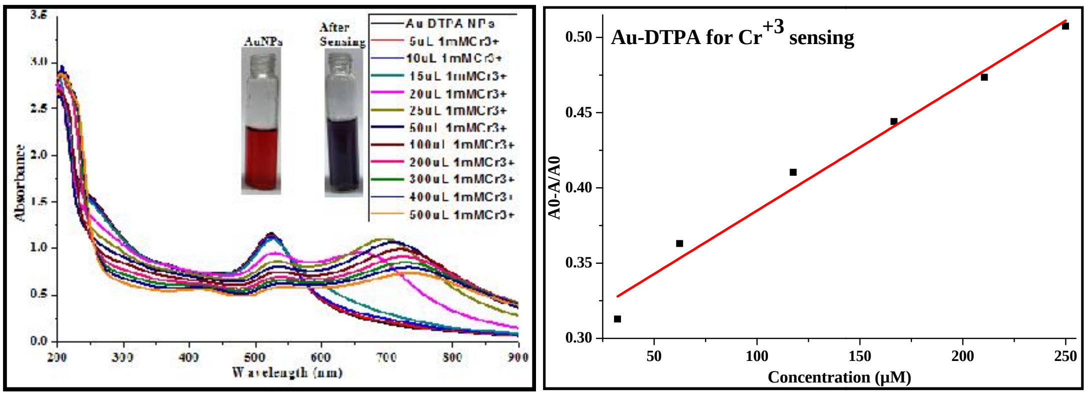

Figure 5.13(a) concentration variation studies for Cr^{3+}-AuNPs-DTPA sensing

(b) linear plot of Cr^{+3} sensing using Au-DTPA

Figure 5.13a shows the SPR absorption change with the addition of different amount of Cr^{3+}. The absorbance at 520 nm decreased with increasing Cr^{3+} concentration. A new band at 700±50 nm formed during Cr^{3+} titration as a result of the induced aggregation of AuDTPA NPs. A linear relationship was found when the concentration of Cr^{3+} ions was between 5uL and 500uL of 1M of Cr^{3+} solution on plotting a calibration graph for Cr^{3+} as described under section 5.4.2.1.

The limit of detection for Cr^{3+} was found to be 2.38 uM with the linear range 32.26 - 250 μM (Figure 5.13b). The shift in the surface plasmon resonance peak for AuNPs was the result of the charge-based interaction between the negatively charged groups of chromium $Cr(OH)_4^-$ and positively charged groups of AuNPs DTPA (NR_3^+) as well as hydrogen bonding between $Cr(OH)_4^-$ and COO^- groups of AgDTPA

5.4.3.2 Au-DTPA NPs - Calibration plot for Cr^{6+}

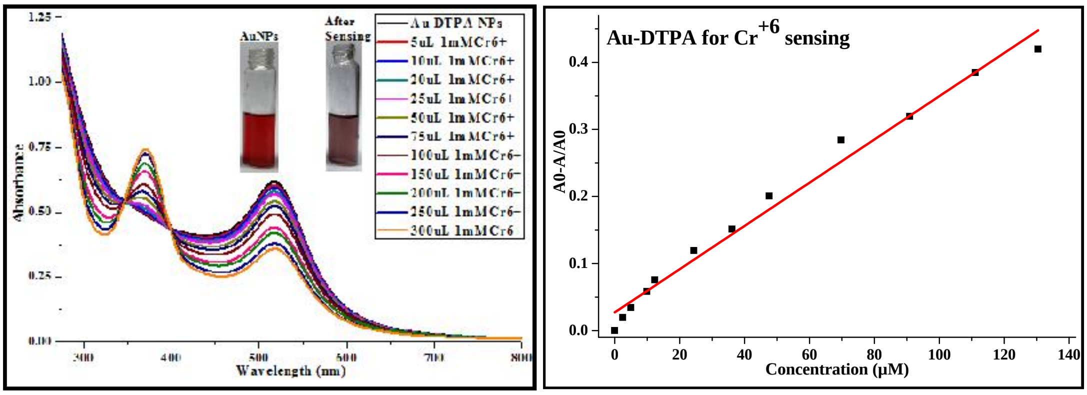

Figure 5.14(a) concentration variation studies for Cr^{6+}-AuNPs-DTPA sensing (b) linear plot of Cr^{+6} sensing using Au-DTPA

The initial Au-DTPA NPs exhibit SPR absorption peak at 520 nm. As the concentration of Cr^{6+} increases, the absorbance decreases at 520nm and increases at 370 nm. The two isobestic points represent the CrO_4^{2-} and $HCrO_4^-$ components in equilibrium (Cruywagen, Heyns, & Rohwer, 1998). The limit of detection for Cr^{6+} was found to be 1.79 µM with the linear range 2.5µM-130 µM (Figure 5.14b) when a calibration graph for Cr^{6+} was plotted as described under section 5.4.2.1 after addition of Cr^{6+} solution of different concentrations..

5.4.3.3 Au-DTPA NPs- Effect of other metal on sensing (Cr^{3+}/Cr^{6+})

The selectivity studies towards Cr^{3+} and Cr^{6+} in presence of other metal ions were carried out. For this, the concentrations of metal ions were taken 1mM.

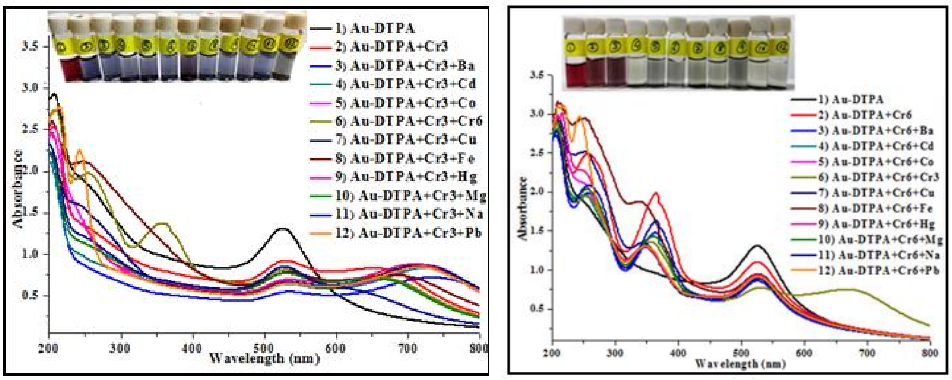

Figure 5.15 (a) Au-DTPA NPs Effect of other metal on sensing in presence of Cr^{3+} (b) Au-DTPA NPs: Effect of other metal on sensing in presence of Cr^{6+}

Interference studies for influence of other metal ions on Cr^{3+} binding to Au-DTPA NPs, competitive experiments were carried out in the presence of Cr^{3+}(1 mM) with other metal ions Ba^{2+}, Cd^{2+}, Co^{2+}, Cu^{2+}, Hg^{2+}, Mg^{2+}, Na^{+}, Pb^{2+} and Cr^{6+} at 1mM each (Figure 5.15a). The SPR absorption shift caused by the mixture of Cr^{3+} with another metal ion was similar to that caused solely by Cr^{3+} except Cr^{6+}. This indicates that other metal ions except Cr^{6+} did not interfere in the binding of Au-DTPA NPs with Cr^{3+}.

The selectivity of the AuDTPA NPs reponse towards Cr^{6+} was also evaluated by testing its response towards 1 mM Cr^{6+} in the presence of 1mM concentrations of other environmentally relevant ions under optimum conditions. Cr^{3+} was the only ion that resulted in an absorption peak shift ($\Delta\lambda_{max}$), This red shift could also be observed by the naked eye as a colour change from red to blue. Fe^{3+} and Cu^{2+} had mild interference.

5.5 Raman Analysis

5.5.1 Raman Analysis of Ag-DTPA

Surface enhanced Raman spectroscopy (SERS) is a powerful analytical method and was used to investigate the capping on DTPA capped AgNPs in aqueous media as well as their interaction with chromium.The Raman Spectra of Au and Ag DTPA NPs are shown in Figures 5.6 and 5.7 respectively and the assignments to the various vibrations are tabulated in tables 5.1 and 5.2 respectively.

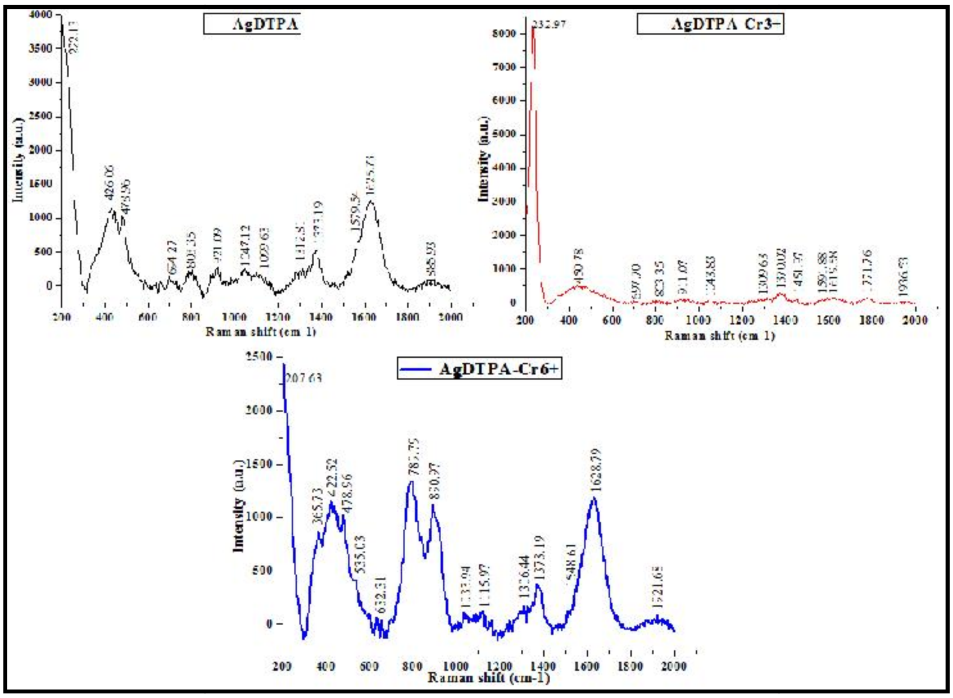

Figure 5.16 Raman Analysis for Ag DTPA

As seen from Figure 5.16, the intense shoulder at 222.13 cm^{-1} is attributed to the stretching vibrations of Ag-O bonds (Kora, Beedu, & Jayaraman, 2012) indicating the formation of an ionic bond between silver and carboxylate. In AgDTPA-Cr^{3+} sharper intense Raman bands were observed at 232.97 cm^{-1} which represents the Ag-O vibration while in AgDTPA-Cr^{6+} it again appears as a shoulder. In AgDTPA-Cr^{6+} the band at 365.73 cm^{-1} could be attributed to O-Cr-O in-plane bending strongly coupled to C-C-C and C-CH_3 in-plane bending vibrations (Dolati, Tayyari, Vakili, & Ebrahimi, 2016). The bands at 535.03 and 632.31 cm^{-1} were attributed to Cr^{3+} species in AgDTPA-Cr^{3+} with significant contributions from a -Cr-OOH (Hurley & McCreery, 2003). The broad peaks at 1373.19 cm^{-1} in AgDTPA and AgDTPA-Cr^{6+} and at 1370.02 cm^{-1} in AgDTPA-Cr^{3+} corresponded to the symmetric stretches of carboxylate group respectively (Kizil, Irudayaraj, & Seetharaman, 2002). The peak at 1625.73 cm^{-1} results from the asymmetric stretching mode of ionized carboxylate groups which was reduced in intensity in Cr^{3+} at 1619.58 cm^{-1} indicating interaction of surface bound DTPA molecules with Cr^{3+} but of same intensity in Cr^{6+} at 1628.79 cm^{-1} as well as due to Raman active water band (Nuttall & Stalker, 1976). This confirmed the capping of DTPA on silver and symmetrical COO- stretching vibrations cause peaks 1451.97 cm^{-1} in AgDTPA-Cr^{3+} which was very weak in AgDTPA and Ag DTPA-Cr^{6+}.. The peak at 1885.93 cm^{-1} in AgDTPA and 1771.76 cm^{-1} in AgDTPA-Cr^{3+} could be attributed to C=O of free acid (Riri et al., 2011) while 1115.97 cm^{-1} band in AgDTPA-Cr^{6+} could be attributed to C-N stretch.

Free Cr^{6+} ion in 0.5 mol/l of potassium dichromate solution had a characteristic peak at 903.3 cm^{-1} (Z. Ren et al., 2016). The peak at 789.79 cm^{-1} for Cr^{6+} could be attributed to binding of Cr^{6+} to DTPA in Cr^{6+} Cr-O stretch AgDTPA (Mosier-Boss & Putnam, 2013; Weckhuysen & Schoonheydt, 1999). Peaks at 1936.53 and 1921.68 cm^{-1} due to bound C=O group in AgDTPA-Cr^{3+} and AgDTPA-Cr^{6+}. In AgDTPA-Cr^{3+} 697.70cm^{-1} is attributed to CrO_6 octahedron.

Table 5.1 Raman spectral analysis for AgDTPA-NPs/ AgDTPA-Cr^{3+}/ AgDTPA-Cr^{6}

Sample	RamanShift (cm^{-1})	Interpretation
Ag DTPA	222.13	Ag-O stretching vibration
	694.27	Ag-OH stretching vibration
	921.09	C-C bond stretching vibrations
	1047.12	C-H in plane bending
	1312.81	C-H deformations
	1373.19	the symmetric stretches of carboxylate
	1579.54	vibrations of water molecule antisymmetrical COO- stretching mode
AgDTPA-Cr^{3+}	232.97	the Ag-O vibration
	450.78	Cr-O stretching
	911.07	C-C bond stretching vibrations
	1043.83	C-H in plane bending
	1309.63	C-H deformations
	1370.02	the symmetric stretches of carboxylate
	1591.88	vibrations of water molecule , antisymmetrical COO- stretching mode, NH+ bending
AgDTPA-Cr^{6+}	207.63	the Ag-O vibration
	365.73	O-Cr-O in-plane bending
	422.52	Cr-O stretching
	890.97	C-C bond stretching vibrations
	1033.94	C-H in plane bending
	1306.44	C-H deformations
	1373.19	the symmetric stretches of carboxylate
	1548.61	vibrations of water molecule and the antisymmetrical COO- stretching mode, NH+ bending

5.5.2 Raman Analysis of Au-DTPA

Gold does not have any intrinsic raman band (Figure 5.17). In Au-DTPA broad peaks at 1351 cm^{-1} and 1545.51 cm^{-1} correspond to the symmetric and asymmetric C=O stretching vibrations of carboxylate group respectively (Kizil et al., 2002) while ca. 418.99cm^{-1} and 482.47 cm^{-1} are associated with the δ(C-C) vibrations in AuDTPA.

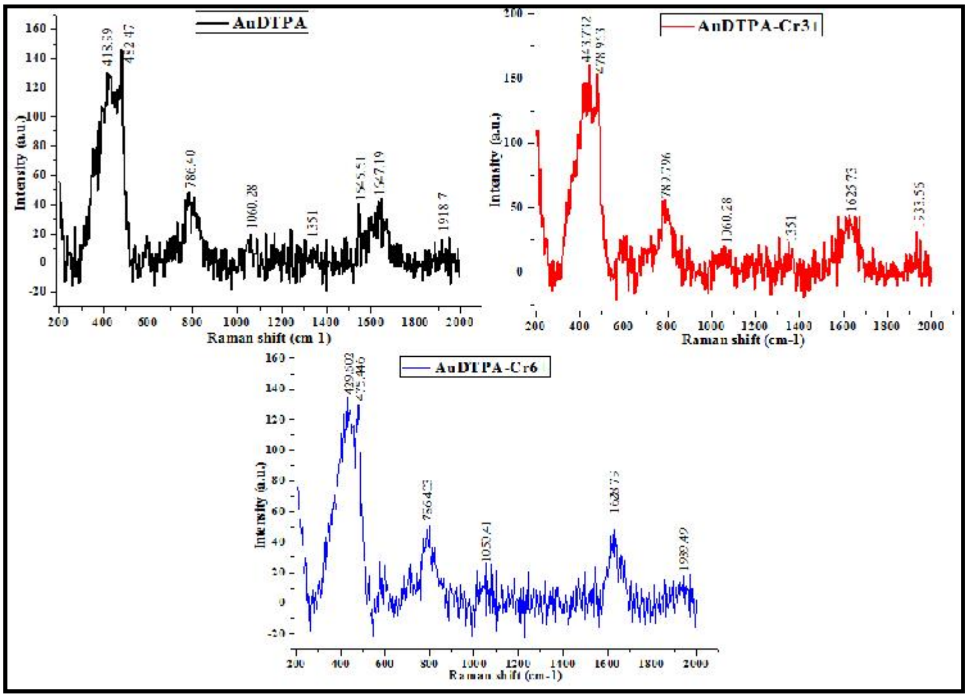

Figure 5.17 Raman Analysis for Au-DTPA

The band at 443.73 cm^{-1} was attributed to Cr-O stretching in Cr^{3+} and at 429.60 in Cr^{6+}. The bands at 478.96 and 475.44 to Au-O in AuDTPA-Cr^{3+} and AuDTPA-Cr^{6+}.

Table 5.2 Raman spectral analysis for AuDTPA / AuDTPA-Cr^{3+}/ AuDTPA-Cr^{6} NPs

Sample	RamanShift (cm^{-1})	Interpretation
Au DTPA	786.4	C-H/C=O out of plane wag
	1060.28	C-H in plane bending
	1351	symmetric C=O stretching vibrations of carboxylate
	1545.51	asymmetric C=O stretching vibrations of carboxylate
	1647.19	asymmetric stretching mode of ionized carboxylate groups
	1918.7	C=O of free acid
	418.99; 482.47	δ(C-C) vibrations
AuDTPA-Cr^{3+}	443.73	Cr-O stretching
	478.96	Au-O, NH+ stretching
	789.79	C-H/C=O out of plane wag
	1060.28	C-H in plane bending
	1576.46	-NH+ bending
	1625.73	asymmetric stretching mode of ionized carboxylate groups
	1933.56	bound C=O group
AuDTPA-Cr^{6+}	429.6	Cr-O stretching
	475.44	Au-O
	786.4	C-H/C=O out of plane wag
	1050.41	C-H in plane bending
	1542.41	-NH+ bending, asymmetric C=O stretching vibrations of carboxylate
	1628.7	asymmetric stretching mode of ionized carboxylate groups
	1939.49	bound C=O group

The peak at 1647.19 cm^{-1} resulted from the asymmetric stretching mode of ionized carboxylate groups which was reduced in intensity in Cr^{3+} at 1625.73 cm^{-1} and

Cr^{6+} at 1628.79 cm^{-1} indicating interaction of surface bound DTPA molecules with Cr^{3+} and Cr^{6+}. The peak at 1918.70 **c**m^{-1} in AuDTPA can be attributed to C=O of free acid (Riri et al., 2011). The band at 1933.56 cm^{-1} and 1939.49 cm^{-1} due to bound C=O group in AuDTPA-Cr^{3+} and AuDTPA-Cr^{6+}. The band at 443.73 cm^{-1} was attributed to Cr-O stretching in AuDTPA-Cr^{3+} and at 429.6 cm^{-1} in AuDTPA-Cr^{6+}.

5.6. Mechanism

DTPA forms complex with silver ions. The reduction of Ag+ ions occurs without adding any other reducing agent as these complexing ligands with their carboxyl groups deprotonated are electron donors and can undergo redox reactions (Yang & Sardar, 2011). Thus, it seems that in the present case that anionic DTPA reduces Ag+ ion, Furthermore since the reduction of AgNPs occurs at pH 8.0 Ag2O might also be playing a role in facilitating the reduction of Ag^+ (Jacob, Mahal, Biswas, Mukherjee, & Kapoor, 2008). There are electrostatic interactions between the deprotonated carboxylate and the protonated amino group among DTPA molecules at pH 7 to 8, so this interaction facilitates the crosslinking of the particles and chain-like network is mainly dominant. Thus the formed silver nano particles are electrostatically stabilized by carboxylate ligands (Chadha et al., 2014). The steric repulsion between the capped molecules contributes to the stability of nanoparticles.

DTPA which is seen to have good reducing properties was also able to reduce HAuCl4 to form gold nano particles.HAuCl4 could be reduced to gold by typical redox process as observed for NTA (Njagi & Goia, 2014) and citrate (Carr, Kelter, & Ericson, 1981). It was observed in section 5.3.2.2 that excess of DTPA was required to obtain stable gold nano particles wherein the carboxylic group in the molecule to strongly attach to the surface of gold nanoparticles as also observed in the case of citrate and NTA and also prevent interatom interaction among the gold nanoparticles (Njagi & Goia, 2014) and citrate (Carr et al., 1981). As DTPA concentration was increased more efficient formation of AuNPS occurred.

At pH 7 and 8 the pH conditions during treatment of silver and gold nanoparticles with chromium, Cr^{3+} exists as $Cr(OH)_4^-$ species (Matović, Jeremić, Jelić, Zlatar, & Jakovljević, 2013) and Cr^{6+} exists as $HCrO_4^-$ (Arar & Pfaff, 1991). These species can interact through hydrogen bonds via carboxylate groups and coordinated water molecules with DTPA. Further there can be ionic interaction with protonated amino group of DTPA. The aggregation of Ag/AuDTPA nanoparticles cannot be due to formation of $[CrDTPA(H_2O)]^{2-}$ complex as its absorption maxima appeared at 552 and 387 nm in aqueous solutions (Ali & Sulfab, 2012). The interaction between Cr^{3+} as well as Cr^{6+} with DTPA may be strong enough weakening the protective capping of Ag/Au colloids and hence aggregation of the nano particles.

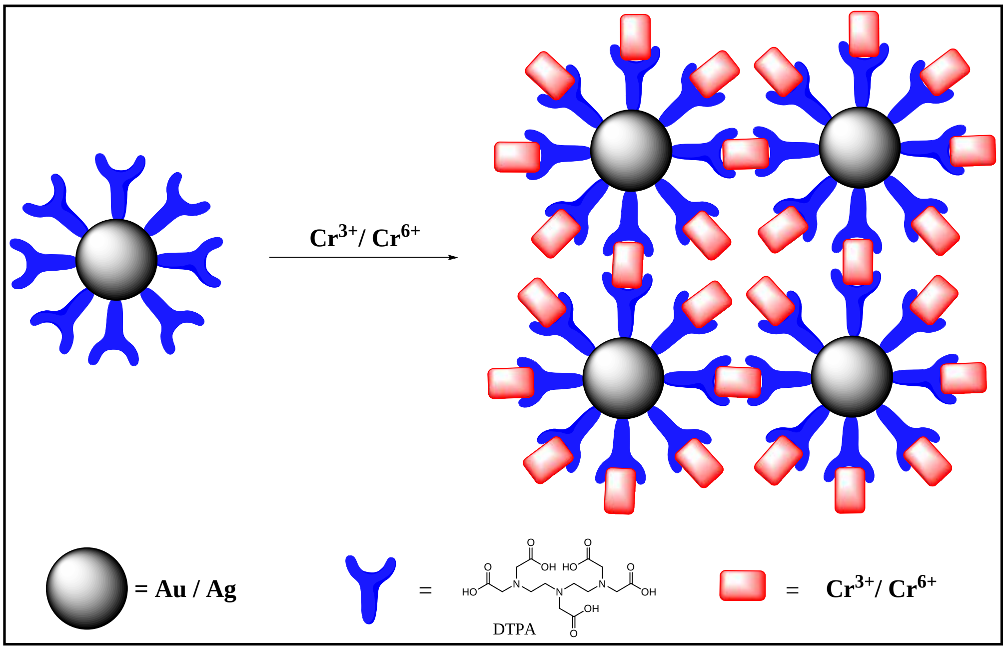

Figure 5.18 Mechanisam

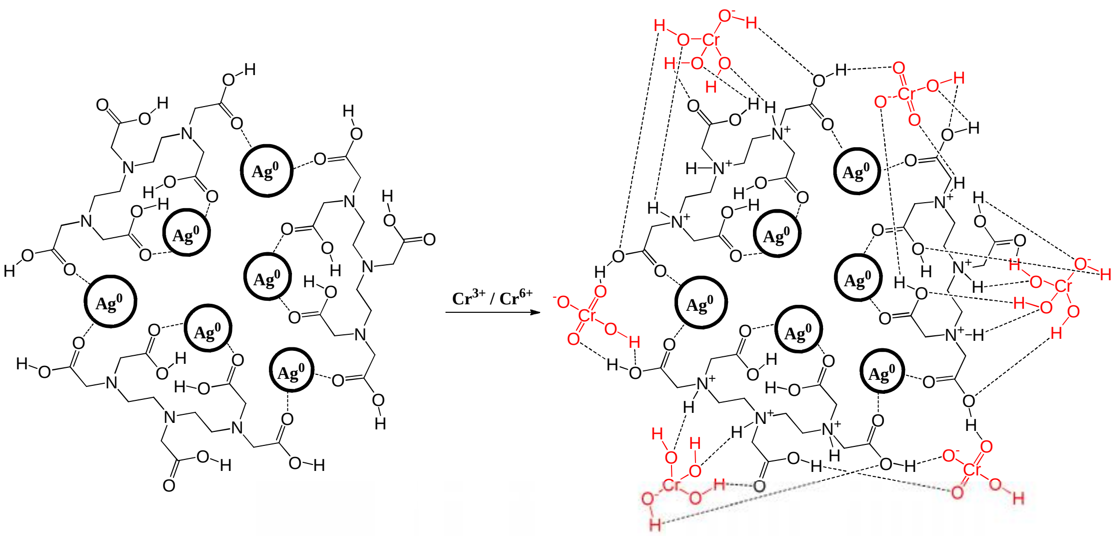

$$DTPA + M^{n+} \longrightarrow oxidised\ species + M^0$$

$$M^0 + M^{n+} \xrightarrow{fast} M_2^{n+}\ (Growth)$$

$$M_2^{n+} + M_2^{n+} \xrightarrow{fast} M_4^{2n+}\ (Growth)$$

$$(M_4^{2n+})_n + (DTPA)_n \xrightarrow{fast} Yellow\ (Ag)/Red\ (Au)\ \ (electrostatic\ attractiattraction)$$

(AgNPs, λ_{max}=400 nm / AuNPs, λ_{max}=520 nm)

5.7. Conclusions

The prepared nanoparticles have several advantages, including (i) simple and low-cost preparation; (ii) high selectivity and sensitivity to Cr^{3+}/Cr^{6+} with reasonable detection limi; (iii) displaying a marked red-shift in the UV-vis extinction spectra and a visible color change was observed; and (iv) detection of Cr^{3+} in aqueous solution, excluding the need for any organic solvent. The essential advantage of liquid state synthesis is the formation of uniform AgNPs having certain particle size through selective synthesis.The recent literature reports of the use of capped Ag and Au NPs are tabulated in **Table 5.3**

Table 5.3 Literature reported Au/AgNPs for detecting Cr^{3+}/ Cr^{6+}

Nano-particles	Capping Agent	Size (nm)	Analyte	LOD	References
Au	Triazole	14	Cr^{3+}	1.4µM	(Y. C. Chen, Lee, Sung, & Wu, 2013)
Au	TNBA-HP	15	Cr^{3+}	0.04µM	(Zhou et al., 2012)
Au	TNBA	-	Cr^{3+}	1µM	(Lai & Tseng, 2011)
Au	DTNBA	13	Cr^{3+}	(93.6ppb) 0.093 µM	(Dang, Li, Wang, Li, & Wu, 2009)
Au	Citrate	13.8	Cr^{3+}	4.0µM	(Liu & Wang, 2013)
Au	Tripolyphosphate	11.13	Cr^{3+}	0.1 µM	(Xin, Miao, Chen, & Wu, 2012)
Au	BP-DTC Dithiocarbamate - modified Nbenzyl-4-(pyridin-4-ylmethyl)aniline ligand	-	Cr^{3+}	0.6µM (31ppb)	(Zhao et al., 2012)
Au	Citrate	30-35	Cr^{3+}	0.022µM	(Elavarasi, Rajeshwari, Chandrasekaran, & Mukherjee, 2013)
Au	Meso-2,3-dimercaptosucci nic acid	14	Cr^{3+} Cr^{6+}	0.01 µM	(W. Chen et al., 2015)
Au	EDTA	6	Cr^{3+}	0.08 µM	(J. Li, Du, & Zhang, 2014)
Au	Tween 20	13	Cr^{3+} Cr^{6+}	0.016 µM 0.009 µM	(X. Wang, Wei, Wang, & Chen, 2015)
Au	4-CBUAB-polymerized vesicles	32	Cr^{3+}	0.72 ug/L	(Kapakoglou, Giokas, Tsogas, Ladavos, & Vlessidis, 2009)
Au		-	Cr^{6+}	0.1 µM (8.8×10^{-8} M)	(F. M. Li et al., 2011)
Au	Borohydride	3.9nm	Cr^{3+}	1.34×10^{-8} M (13.42nM)	(Shellaiah, Simon, Sun, & Ko, 2016)
Ag	Sodium borohydride	65±2	Cr^{3+}	2×10^{-9}M	(Elavarasi et al., 2012)
Ag	Ascorbic acid		Cr^{6+}	0.07 µM 5×10^{-8} M	(Wu, Xu, Dong, Jiang, & Zhu, 2013)
Ag	MNA and MA	5	Cr^{3+}	64.51×10^{-9} nM	(Modi, Mehta, & Kailasa, 2014)
Ag_{core}-Au_{shell}	CTAB	-	Cr^{6+}	0.01 µM (1×10^{-7}M)	(Xin, Zhang, et al., 2012)
AuDTPA	DTPA	19-30	Cr^{3+}	2.38 µM	Present work
			Cr^{6+}	1.79 µM	
AgDTPA	DTPA	7-13	Cr^{3+}	1.62 µM	
			Cr^{6+}	1.77 µM	

It can be seen that the DTPA capped Au and Ag NPs under study are comparable with triazole, DNBA and citrate capped AuNPS while others had better detection limits. However most of the literature reported NPs required a reducing agent in addition to capping agent during synthesis which was not so in the present study. Further the synthesis was done by adopting to green microwaves and nontoxic DTPA. Futhermore most of the literature reported methods require conversion of Cr^{6+} to Cr^{3+} to determine Cr^{6+} which was not necessary in the present study.

References

Ahmadi, T. S., Wang, Z. L., Green, T. C., Henglein, a., & El-Sayed, M. a. (1996). Shape-Controlled Synthesis of Colloidal Platinum Nanoparticles. *Science*. doi:10.1126/science.272.5270.1924

Ali, I. H., & Sulfab, Y. (2012). One-Electron Transfer in the Oxidation of Chromium (III) Complexes with trans-1,2-N, N,N,N-tetraacetate and Diethylenetriamine-pentaacetate Ligands by Periodate Ion. *International Journal of Chemical Kinetics*, *44*(11), 729–735. doi:10.1002/kin.20723

Andreescu, D., Sau, T. K., & Goia, D. V. (2006). Stabilizer-free nanosized gold sols. *Journal of Colloid and Interface Science*, *298*(2), 742–751. doi:http://dx.doi.org/10.1016/j.jcis.2006.01.011

Arakawa, R., & Kawasaki, H. (2010). Functionalized nanoparticles and nanostructured surfaces for surface-assisted laser desorption/ionization mass spectrometry. *Analytical Sciences : The International Journal of the Japan Society for Analytical Chemistry*, *26*(12), 1229–1240. doi:10.2116/analsci.26.1229

Arar, E. J., & Pfaff, J. D. (1991). Determination of dissolved hexavalent chromium in industrial wastewater effluents by ion chromatography and post-column derivatization with diphenylcarbazide. *Journal of Chromatography A*, *546*(C), 335–340. doi:10.1016/S0021-9673(01)93031-6

Bahadur, N. M., Furusawa, T., Sato, M., Kurayama, F., Siddiquey, I. A., & Suzuki, N. (2011). Fast and facile synthesis of silica coated silver nanoparticles by microwave irradiation. *Journal of Colloid and Interface Science*, *355*(2), 312–320. doi:10.1016/j.jcis.2010.12.016

Bai, Z., Chen, R., Si, P., Huang, Y., Sun, H., & Kim, D. H. (2013). Fluorescent pH sensor based on Ag@SiO2 core-shell nanoparticle. *ACS Applied Materials and Interfaces*, *5*(12), 5856–5860. doi:10.1021/am401528w

Bonggotgetsakul, Y. Y. N., Cattrall, R. W., & Kolev, S. D. (2011). The preparation of a gold nanoparticle monolayer on the surface of a polymer inclusion membrane using {EDTA} as the reducing agent. *Journal of Membrane Science*, *379*(1–2), 322–329. doi:http://dx.doi.org/10.1016/j.memsci.2011.06.003

Brust, M., Walker, M., Bethell, D., Schiffrin, D. J., & Whyman, R. (1994). Synthesis of thiol-derivatised gold nanoparticles in a two- phase Liquid – Liquid system. *Journal of the Chemical Society, Chemical Communications*, *1994*(7), 801–802.

doi:10.1039/C39940000801

Burda, C., Chen, X., Narayanan, R., & El-Sayed, M. A. (2005). Chemistry and properties of nanocrystals of different shapes. *Chemical Reviews*. doi:10.1021/cr030063a

Carr, J. D., Kelter, P. B., & Ericson, A. T. (1981). Ferrate(VI) oxidation of nitrilotriacetic acid. *Environmental Science & Technology*, *15*(2), 184–187. doi:10.1021/es00084a001

Cavicchioli, M., Varanda, L. C., Massabni, A. C., & Melnikov, P. (2005). Silver nanoparticles synthesized by thermal reduction of a silver(I)–aspartame complex in inert atmosphere. *Materials Letters*, *59*(28), 3585–3589. doi:http://dx.doi.org/10.1016/j.matlet.2005.07.001

Chadha, R., Das, A., Maiti, N., & Kapoor, S. (2014). Synthesis of silver nanoparticles: Effects of anionic ligands on formation and catalytic activity. *Materials Chemistry and Physics*, *148*(3), 1124–1130. doi:http://dx.doi.org/10.1016/j.matchemphys.2014.09.031

Chen, W., Cao, F., Zheng, W., Tian, Y., Xianyu, Y., Xu, P., … Jiang, X. (2015). Detection of the nanomolar level of total Cr[(iii) and (vi)] by functionalized gold nanoparticles and a smartphone with the assistance of theoretical calculation models. *Nanoscale*, *7*(5), 2042–9. doi:10.1039/c4nr06726f

Chen, Y. C., Lee, I. L., Sung, Y. M., & Wu, S. P. (2013). Triazole functionalized gold nanoparticles for colorimetric Cr3+ sensing. *Sensors and Actuators, B: Chemical*, *188*, 354–359. doi:10.1016/j.snb.2013.06.088

Cruywagen, J. J., Heyns, J. B. B., & Rohwer, E. A. (1998). New spectrophotometric evidence for the existence of HCrO4−. *Polyhedron*, *17*(10), 1741–1746. doi:http://dx.doi.org/10.1016/S0277-5387(97)00443-9

Dang, Y. Q., Li, H. W., Wang, B., Li, L., & Wu, Y. (2009). Selective detection of trace Cr3+ in aqueous solution by using 5,5’-dithiobis (2-Nitrobenzoic acid)-modified gold nanoparticles. *ACS Applied Materials and Interfaces*, *1*(7), 1533–1538. doi:10.1021/am9001953

Devi, L. S., & Joshi, S. R. (2015). Ultrastructures of silver nanoparticles biosynthesized using endophytic fungi. *Journal of Microscopy and Ultrastructure*, *3*(1), 29–37. doi:http://dx.doi.org/10.1016/j.jmau.2014.10.004

Dolati, F., Tayyari, S. F., Vakili, M., & Ebrahimi, A. (2016). Vibrational spectra of αbromo and α-chloro derivatives of tris(acetylacetonato)chromium(III). *Journal of Molecular Structure*, *1103*, 1–8. doi:http://dx.doi.org/10.1016/j.molstruc.2015.09.012

Elavarasi, M., Paul, M. L., Rajeshwari, A., Chandrasekaran, N., Mandalb, A. B., & Mukherjee, A. (2012). Studies on fluorescence determination of nanomolar Cr(III) in aqueous solutions using unmodified silver nanoparticles. *Analytical Methods*, *4*, 3407–3412. doi:10.1039/c2ay25632k

Elavarasi, M., Rajeshwari, A., Chandrasekaran, N., & Mukherjee, A. (2013). Simple colorimetric detection of Cr(iii) in aqueous solutions by as synthesized citrate capped gold nanoparticles and development of a paper based assay. *Analytical Methods*, *5*(21), 6211–6218. doi:10.1039/C3AY41435C

Guo, R., Zhang, L., Zhu, Z., & Jiang, X. (2008). Direct facile approach to the fabrication of chitosan-gold hybrid nanospheres. *Langmuir*, *24*(7), 3459–3464. doi:10.1021/la703080j

Haiss, W., Thanh, N. T. K., Aveyard, J., & David G. Fernig. (2007). Determination of Size and Concentration of Gold Nanoparticles from UV−Vis Spectra. *Analytical Chemistry*, *79*(11), 4215–4221. doi:10.1021/ac0702084

Hsieh, C.-T., Pan, C., & Chen, W.-Y. (2011). Synthesis of silver nanoparticles on carbon papers for electrochemical catalysts. *Journal of Power Sources*, *196*(15), 6055–6061. doi:http://dx.doi.org/10.1016/j.jpowsour.2011.03.087

Hurley, B. L., & McCreery, R. L. (2003). Raman Spectroscopy of Monolayers Formed from Chromate Corrosion Inhibitor on Copper Surfaces. *Journal of The Electrochemical Society*, *150*(8), B367–B373. doi:10.1149/1.1586923

Jacob, J. A., Mahal, H. S., Biswas, N., Mukherjee, T., & Kapoor, S. (2008). Role of Phenol Derivatives in the Formation of Silver Nanoparticles. *Langmuir*, *24*(2), 528–533. doi:10.1021/la702073r

Ji, X., Song, X., Li, J., Bai, Y., Yang, W., & Peng, X. (2007). Size control of gold nanocrystals in citrate reduction: The third role of citrate. *Journal of the American Chemical Society*, *129*(45), 13939–13948. doi:10.1021/ja074447k

Jiang, D., Chen, L., Zhu, J., Chen, M., Shi, W., & Xie, J. (2013). Novel p-n heterojunction photocatalyst constructed by porous graphite-like C3N4 and nanostructured BiOI: facile synthesis and enhanced photocatalytic activity. *Dalton Transactions (Cambridge, England : 2003)*, *42*(44), 15726–34.

doi:10.1039/c3dt52008k

Jiang, D., Xie, J., Chen, M., Li, D., Zhu, J., & Qin, H. (2011). Facile route to silver submicron-sized particles and their catalytic activity towards 4-nitrophenol reduction. *Journal of Alloys and Compounds*, *509*(5), 1975–1979. doi:10.1016/j.jallcom.2010.10.107

Kapakoglou, N. I., Giokas, D. L., Tsogas, G. Z., Ladavos, A. K., & Vlessidis, A. G. (2009). Development of a chromium speciation probe based on morphology-dependent aggregation of polymerized vesicle-functionalized gold nanoparticles. *The Analyst*, *134*(12), 2475–2483. doi:10.1039/b909619a

Kapoor, S., & Mukherjee, T. (2003). Growth and reactivity of silver clusters in amino polycarboxylic acid solutions. *Journal of Colloid and Interface Science*, *264*(1), 301–306. doi:10.1016/S0021-9797(03)00353-9

Kim, T., Lee, K., Gong, M., & Joo, S.-W. (2005). Control of Gold Nanoparticle Aggregates by Manipulation of Interparticle Interaction. *Langmuir*, *21*(21), 9524–9528. doi:10.1021/la0504560

Kizil, R., Irudayaraj, J., & Seetharaman, K. (2002). Characterization of irradiated starches by using FT-Raman and FTIR spectroscopy. *Journal of Agricultural and Food Chemistry*, *50*(14), 3912–3918. doi:10.1021/jf011652p

Kora, A., Beedu, S., & Jayaraman, A. (2012). Size-controlled green synthesis of silver nanoparticles mediated by gum ghatti (Anogeissus latifolia) and its biological activity. *Organic and Medicinal Chemistry Letters*, *2*(1), 17. doi:10.1186/2191-2858-2-17

Lai, Y.-J., & Tseng, W.-L. (2011). Role of 5-thio-(2-nitrobenzoic acid)-capped gold nanoparticles in the sensing of chromium(vi): remover and sensor. *The Analyst*, *136*(13), 2712–2717. doi:10.1039/c1an15162b

Li, F. M., Liu, J. M., Wang, X. X., Lin, L. P., Cai, W. L., Lin, X., … Lin, S. Q. (2011). Non-aggregation based label free colorimetric sensor for the detection of Cr (VI) based on selective etching of gold nanorods. *Sensors and Actuators, B: Chemical*, *155*(2), 817–822. doi:10.1016/j.snb.2011.01.054

Li, H., Cui, Z., & Han, C. (2009). Glutathione-stabilized silver nanoparticles as colorimetric sensor for Ni2+ ion. *Sensors and Actuators, B: Chemical*, *143*(1), 87–92. doi:10.1016/j.snb.2009.09.013

Li, H., Yao, Y., Han, C., & Zhan, J. (2009). Triazole-ester modified silver nanoparticles: click synthesis and Cd2+ colorimetric sensing. *Chemical Communications (Cambridge, England)*, (32), 4812–4814. doi:10.1039/b908761c

Li, J., Du, J., & Zhang, J. (2014). Ethylenediaminetetraacetic acid functionalized gold nanoparticles for sensitive colorimetric detection of chromium(III). *Journal of the Chinese Chemical Society*, *61*(12), 1395–1399. doi:10.1002/jccs.201400139

Liu, Y., & Wang, X. (2013). Colorimetric speciation of Cr(iii) and Cr(vi) with a gold nanoparticle probe. *Analytical Methods*, *5*(6), 1442–1448. doi:10.1039/C3AY00016H

Matović, Z. D., Jeremić, M. S., Jelić, R. M., Zlatar, M., & Jakovljević, I. Ž. (2013). Configurational, {LFDFT} and {NBO} analysis of chromium(III) complexes of edta-type ligands. *Polyhedron*, *55*, 131–143. doi:http://dx.doi.org/10.1016/j.poly.2013.02.079

Mie, G. (1908). Beitrzur Optik truber Medien, speziell kolloidaler Metallosungen. *Annalen Der Physik*, *330*(3), 377–445. doi:10.1002/andp.19083300302

Modi, R. P., Mehta, V. N., & Kailasa, S. K. (2014). Bifunctionalization of silver nanoparticles with 6-mercaptonicotinic acid and melamine for simultaneous colorimetric sensing of Cr3+ and Ba2+ ions. *Sensors and Actuators, B: Chemical*, *195*, 562–571. doi:10.1016/j.snb.2014.01.059

Mosier-Boss, P. A., & Putnam, M. D. (2013). Detection of hexavalent chromium using gold/4-(2-mercaptoethyl) pyridinium surface enhanced Raman scattering-active capture matrices. *Analytica Chimica Acta*, *801*, 70–77. doi:http://dx.doi.org/10.1016/j.aca.2013.09.006

Njagi, J. I., & Goia, D. V. (2014). Nitrilotriacetic acid: A novel reducing agent for synthesizing colloidal gold. *Journal of Colloid and Interface Science*, *421*, 27–32. doi:http://dx.doi.org/10.1016/j.jcis.2014.01.025

Nuttall, R. H., & Stalker, D. M. (1976). The Raman spectra of protonated EDTA metal complexes. *Inorganic and Nuclear Chemistry Letters*, *12*(8), 639–641. doi:http://dx.doi.org/10.1016/0020-1650(76)80083-9

Pal, T., Sau, T. K., & Jana, N. R. (1998). Silver Hydrosol, Organosol, and Reverse Micelle-Stabilized Sol--A Comparative Study. *Journal of Colloid and Interface Science*, *202*(1), 30–36. doi:10.1006/jcis.1997.5353

Rattanarat, P., Dungchai, W., Cate, D. M., Siangproh, W., Volckens, J., Chailapakul, O., & Henry, C. S. (2013). A microfluidic paper-based analytical device for rapid quantification of particulate chromium. *Analytica Chimica Acta*, *800*, 50–55. doi:10.1016/j.aca.2013.09.008

Ren, W., Zhu, C., & Wang, E. (2012). Enhanced sensitivity of a direct SERS technique for Hg2+ detection based on the investigation of the interaction between silver nanoparticles and mercury ions. *Nanoscale*, *4*, 5902–5909. doi:10.1039/c2nr31410j

Ren, Z., Xu, X., Wang, X., Gao, B., Yue, Q., Song, W., … Wang, H. (2016). FTIR, Raman, and XPS analysis during phosphate, nitrate and Cr(VI) removal by amine cross-linking biosorbent. *Journal of Colloid and Interface Science*, *468*, 313–323. doi:http://dx.doi.org/10.1016/j.jcis.2016.01.079

Riri, M., Hor, M., Kamal, O., Eljaddi, T., Benjjar, A., & Hla??bi, M. (2011). New gadolinium(III) complexes with simple organic acids (oxalic, glycolic and malic acid). *Journal of Materials and Environmental Science*, *2*(3), 303–308. doi:10.4161/onci.23288

Shankar, S., & John, S. A. (2015). 4-Amino-6-hydroxy-2-mercaptopyrimidine capped gold nanoparticles as fluorophore for the ultrasensitive and selective determination of l-cysteine. *Sensors and Actuators B: Chemical*, *221*, 1202–1208. doi:http://dx.doi.org/10.1016/j.snb.2015.07.092

Shellaiah, M., Simon, T., Sun, K. W., & Ko, F. H. (2016). Simple bare gold nanoparticles for rapid colorimetric detection of Cr3+ ions in aqueous medium with real sample applications. *Sensors and Actuators, B: Chemical*, *226*, 44–51. doi:10.1016/j.snb.2015.11.123

Shelley, E. J., Ryan, D., Johnson, S. R., Couillard, M., Fitzmaurice, D., Nellist, P. D., … Preece, J. A. (2002). Dialkyl sulfides: Novel passivating agents for gold nanoparticles. *Langmuir*, *18*(5), 1791–1795. doi:10.1021/la0109260

Shevchenko, G. P., Zhuravkov, V. A., & Novikov, A. G. (2015). Proceedings of international conference nanomeeting – 2015. In C. H. K. V E Borisenko, S V Gaponenko, V S Gurin (Ed.), *Physics, Chemistry and Apllications of Nanostructures 2015* (pp. 284–285). Minsk, Belarus. doi:10.1017/CBO9781107415324.004

Svanedal, I., Boija, S., Almesåker, A., Persson, G., Andersson, F., Hedenström, E., … Edlund, H. (2014). Metal Ion Coordination, Conditional Stability Constants, and Solution Behavior of Chelating Surfactant Metal Complexes. *Langmuir*, *30*(16), 4605–4612. doi:10.1021/la5002336

Tzhayik, O., Sawant, P., Efrima, S., Kovalev, E., & Klug, J. T. (2002). Xanthate capping of silver, copper, and gold colloids. *Langmuir*, *18*(8), 3364–3369. doi:10.1021/la015653n

Wang, D. ., Liu, Y., Zhou, X. ., Sun, J. ., & You, T. . (2007). EDTA-controlled One-pot Preparation of Novel Shaped Gold Microcrystals and Their Application in Surface-enhanced Raman Scattering. *Chemistry Letters*, *36*(7), 924–925. doi:10.1246/cl.2007.924

Wang, X., Chen, L., & Chen, L. (2014). Colorimetric determination of copper ions based on the catalytic leaching of silver from the shell of silver-coated gold nanorods. *Microchimica Acta*, *181*(1-2), 105–110. doi:10.1007/s00604-013-1075-7

Wang, X., Wei, Y., Wang, S., & Chen, L. (2015). Red-to-blue colorimetric detection of chromium via Cr (III)-citrate chelating based on Tween 20-stabilized gold nanoparticles. *Colloids and Surfaces A: Physicochemical and Engineering Aspects*, *472*, 57–62. doi:10.1016/j.colsurfa.2015.02.033

Wang, Y., Yan, B., & Chen, L. (2013). SERS Tags: Novel optical nanoprobes for bioanalysis. *Chemical Reviews*. doi:10.1021/cr300120g

Weckhuysen, B. M., & Schoonheydt, R. A. (1999). Olefin polymerization over supported chromium oxide catalysts. *Catalysis Today*, *51*(2), 215–221. doi:http://dx.doi.org/10.1016/S0920-5861(99)00046-2

Wrzesien, J., & Graham, D. (2012). Synthesis of SERS active nanoparticles for detection of biomolecules. *Tetrahedron*, *68*(4), 1230–1240. doi:10.1016/j.tet.2011.11.053

Wu, X., Xu, Y., Dong, Y., Jiang, X., & Zhu, N. (2013). Colorimetric determination of hexavalent chromium with ascorbic acid capped silver nanoparticles. *Anal. Methods*, *5*(2), 560–565. doi:10.1039/C2AY25989C

Xin, J., Miao, L., Chen, S., & Wu, A. (2012). Colorimetric detection of Cr3+ using tripolyphosphate modified gold nanoparticles in aqueous solutions. *Analytical Methods*, *4*, 1259. doi:10.1039/c2ay25061f

Xin, J., Zhang, F., Gao, Y., Feng, Y., Chen, S., & Wu, A. (2012). A rapid colorimetric detection method of trace Cr (VI) based on the redox etching of Agcore-Aushell nanoparticles at room temperature. *Talanta*, *101*, 122–127.

doi:10.1016/j.talanta.2012.09.009

Xiong, D., & Li, H. (2008). Colorimetric detection of pesticides based on calixarene modified silver nanoparticles in water. *Nanotechnology*, *19*(46), 465502. doi:10.1088/0957-4484/19/46/465502

Xu, S., Cao, Y., Zhou, J., Wang, X., Wang, X., & Xu, W. (2011). Plasmonic enhancement of fluorescence on silver nanoparticle films. *Nanotechnology*, *22*(27), 275715. doi:10.1088/0957-4484/22/27/275715

Xu, Y., Yang, X., Zhu, S., & Dou., Y. (2014). Selectively fluorescent sensing of Cu2+ based on lysine-functionalized gold nanoclusters. *Colloids and Surfaces A: Physicochemical and Engineering Aspects*, *450*(1), 115–120. doi:10.1016/j.colsurfa.2014.03.027

Yang, J. H., & Sardar, D. K. (2011). One-Pot Synthesis of Coral-Shaped Gold Nanostructures for Surface-Enhanced Raman Scattering. *Journal of Nano Research*, *14*, 47–55. doi:10.4028/www.scientific.net/JNanoR.14.47

Yao, Y., Tian, D., & Li, H. (2010). Cooperative binding of bifunctionalized and click-synthesized silver nanoparticles for colorimetric Co2+ Sensing. *ACS Applied Materials and Interfaces*, *2*(3), 684–690. doi:10.1021/am900741h

Yi, Q., Niu, F., Li, L., Du, R., Zhou, Z., & Liu, X. (2011). Novel nanoporous silver particles for electro-reduction of hydrogen peroxide in alkaline media. *Journal of Electroanalytical Chemistry*, *654*(1–2), 60–65. doi:http://dx.doi.org/10.1016/j.jelechem.2011.01.031

Yonezawa, T., & Kunitake, T. (1999). Practical preparation of anionic mercapto ligand-stabilized gold nanoparticles and their immobilization. In *Colloids and Surfaces A: Physicochemical and Engineering Aspects* (Vol. 149, pp. 193–199). doi:10.1016/S0927-7757(98)00309-4

Zainy, M., Huang, N. M., Kumar, S. V., Lim, H. N., Chia, C. H., & Harrison, I. (2012). Simple and scalable preparation of reduced graphene oxide–silver nanocomposites via rapid thermal treatment. *Materials Letters*, *89*, 180–183. doi:http://dx.doi.org/10.1016/j.matlet.2012.08.101

Zhang, Q., Li, N., Goebl, J., Lu, Z., & Yin, Y. (2011). A systematic study of the synthesis of silver nanoplates: Is citrate a “magic” reagent? *Journal of the American Chemical Society*, *133*(46), 18931–18939. doi:10.1021/ja2080345

Zhao, L., Jin, Y., Yan, Z., Liu, Y., & Zhu, H. (2012). Novel, highly selective detection of Cr(III) in aqueous solution based on a gold nanoparticles colorimetric assay and its application for determining Cr(VI). *Analytica Chimica Acta*, *731*, 75–81. doi:10.1016/j.aca.2012.04.022

Zhou, Y., Li, Y. S., Tian, X. L., Zhang, Y. Y., Yang, L., Zhang, J. H., … Liu, Z. S. (2012). Enhanced ultrasensitive detection of Cr(III) using 5-thio-2-nitrobenzoic acid (TNBA) and horseradish peroxidase (HRP) dually modified gold nanoparticles (AuNPs). *Sensors and Actuators, B: Chemical*, *161*(1), 1108–1113. doi:10.1016/j.snb.2011.12.035